Apr 27th, 2:00 PM

Technical Paper Session I-B - CIGSeS and CIGS2 Thin Film Solar Cells on Flexible Foils for Space Power

Neelkanth G. Dhere
Florida Solar Energy Center, University of Central Florida

Sachin S. Kulkarni
Florida Solar Energy Center, University of Central Florida

Vinay V. Hadagali
Florida Solar Energy Center, University of Central Florida

Shirish A. Pethe
Florida Solar Energy Center, University of Central Florida

Parag S. Vasekar
Florida Solar Energy Center, University of Central Florida

See next page for additional authors

Presenter Information

Neelkanth G. Dhere, Sachin S. Kulkarni, Vinay V. Hadagali, Shirish A. Pethe, Parag S. Vasekar, Ashwani Kaul, Bhaskar Kumar, and Santosh Khatri

SPACE VISIONS CONGRESS 2007

TECHNICAL PAPER SESSION 1B

"GIGSeS & GIGS2 THIN FILM SOLAR CELLS ON FLEXIBLE FOILS FOR SPACE POWER"

NEELKANTH G. DHERE, ET AL

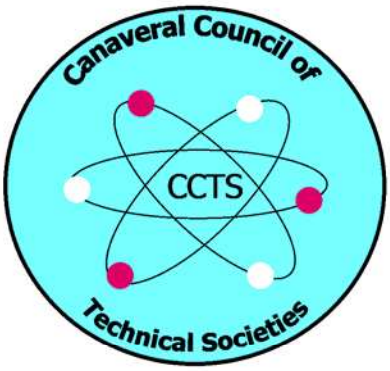

CIGSeS and CIGS2 Thin Film Solar Cells on Flexible Foils for Space Power

Neelkanth G. Dhere, Sachin S. Kulkarni, Vinay V. Hadagali, Shirish A. Pethe, Parag S. Vasekar, Ashwani Kaul, Bhaskar Kumar and Santosh Khatri
Florida Solar Energy Center, University of Central Florida
1679 Clearlake Road, Cocoa, FL 329225703

The objective of the research is to develop flexible, lightweight, radiation-resistant, high-specific-power, highly efficient $CuIn_{1-x}Ga_xSe_{2-y}S_y$ (CIGSeS) and $CuIn_{1-x}Ga_xS_2$ (CIGS2) thin-film solar cells for space electric power. The near optimum bandgap, potential for higher specific power, and superior radiation resistance make this technology an ideal candidate for space electric power. The superior radiation resistance of CIGSeS thin-film solar cells relative to the conventional silicon and gallium arsenide single-crystal cells in the space radiation environment would extend mission lifetimes substantially. The conventional rigid Si and GaAs cells must be folded in an accordion style for deployment space. This can cause problems of opening up and folding of the solar array as has happened recently with the International Space Station. On the other hand, the flexible solar cells and modules can be packaged and rolled out more easily. The stainless steel and titanium foil substrate materials are capable of withstanding high temperatures required for preparing good quality CIGSeS absorber layer. They also do not sag easily and hence do not require rigidizing as is the case with plastic sheet substrates.

The CIGSeS absorber film is prepared by selenization/sulfurization of DC magnetron sputter-deposited CuGa, In metallic precursors on 10 cm x 10 cm metallic foil substrate coated with molybdenum back contact layer. CdS heterojunction partner is deposited by chemical bath deposition. Transparent and conducting bilayer of intrinsic ZnO and aluminum doped ZnO:Al is deposited by RF magnetron sputtering. Cells are completed by depositing Ni/Al front contact fingers by thermal evaporation. The sputtering technique utilized in the preparation of solar cells provides an added advantage of facilitating easy scale-up of the laboratory size cells for economic large-area manufacture by the roll-to-roll process. Chemical composition, crystallographic structure and morphology of CIGSeS thin films are analyzed by energy dispersive spectroscopy, Auger electron spectroscopy, X-ray diffraction, scanning electron microscopy and transmission electron microscopy. The photovoltaic properties of completed cells are studied by measurement of current-voltage characteristics and quantum efficiency. Best efficiencies of 10.4% under AM 1.5 conditions and 8.84% under AM 0 conditions were achieved on small-area CIGS2 thin-film solar cells.

CIGSeS and CIGS2 Thin Film Solar Cells on Flexible Foils for Space Power

Neelkanth G. Dhere
Florida Solar Energy Center
dhere@fsec.ucf.edu

Vivek S. Gade*
Florida Solar Energy Center
gadevivek@yahoo.com

Shantinath R. Ghongadi*
Florida Solar Energy Center
shantinathrg@hotmail.com

Sachin S. Kulkarni
Florida Solar Energy Center
sskulkarni@fsec.ucf.edu

Vinay V. Hadagali
Florida Solar Energy Center
vhadagali@fsec.ucf.edu

Shirish A. Pethe
Florida Solar Energy Center
spethe@fsec.ucf.edu

Parag S. Vasekar
Florida Solar Energy Center
pvasekar@fsec.ucf.edu

Bhaskar Kumar
Florida Solar Energy Center
bbhaskar@fsec.ucf.edu

Ashwani Kaul
Florida Solar Energy Center
akaul@fsec.ucf.edu

Santosh D. Khatri
Florida Solar Energy Center
skhatri@fsec.ucf.edu

Abstract

The work focuses on development of $CuIn_{1-x}Ga_xSe_{2-y}S_y$ *and* $CuIn_{1-x}Ga_xS_2$ *thin film solar cells on lightweight and flexible stainless steel (SS) or titanium foils as substrates. The near optimum bandgap, potential for higher specific power, and superior radiation resistance make this technology an ideal candidate for space electric power. The objective of the present research is to develop lightweight, radiation-resistant, highly efficient, high-specific-power CIGS thin-film solar cells for space electric power. DC magnetron sputtered metallic precursors CuGa/In are selenized/sulfurized. CdS, heterojunction partner, is deposited by chemical bath deposition. Intrinsic ZnO and aluminum doped ZnO are deposited by RF magnetron sputtering followed by Ni/Al front contact fingers by thermal evaporation. Best efficiency of 8.84% under AM 0 conditions and 10.4% under AM 1.5 conditions was achieved on 2.5 cm x 2.5 cm stainless steel substrate from a cell of 0.4* cm^2 *total area.*

1. Introduction

Among the thin film material studied for solar cell applications, $CuIn_{1-x}Ga_xSe_2$ (CIGS) has achieved the highest conversion efficiency of 19.5% [1]. It is a direct bandgap semiconductor having a coefficient of absorption of 3.6×10^5 /cm [2]. The electrically inactive point defects existing in the CIGS material provide inherent p-type conductivity [3]. CIGS solar cells have shown high radiation resistance, compared to crystalline silicon solar cells [4] making it an ideal material for space applications. In comparison to the traditional use of glass substrates, CIGS deposited on thin metal foils advantages of economical large scale roll-to-roll processing, flexibility for very thin foils and improved device cooling under concentration and [5]. Post sulfurization of CIGS is promising for bandgap engineering. Furthermore, it has been reported that the controlled incorporation of sulfur into CIGS films reduces the carrier recombination in the space charge region due to the deep trap states [6]. There is interest in the development of CIGS2 solar cells on flexible substrates. Several groups have reported fabrication of polycrystalline $CuIn_{1-x}Ga_xSe_2$ (CIGS) solar cells on flexible foils substrates [7]. The CIGS cell with an efficiency exceeding 17% has been obtained using SS substrate [8].

The selection of a flexible and lightweight substrate is mainly based on three factors: thermal expansion, chemical effect or the diffusion of detrimental impurities in the absorber layer and the influence of surface properties on nucleation. Titanium

is a potential candidate because its coefficient of thermal expansion is $8.6\times10^{-6}/^{o}C$, close to that of CIGS ($9.0x10^{-6}/^{o}C$). Deposition of SiO_2 on to the Ti substrate prevents the diffusion of impurities and also provides a smooth surface for the growth of an absorber layer. Ti also has high tensile strength and is very stable at selenization and sulfurization temperatures.

Long-term plans envisage swarms of distributed, autonomous, small satellites, termed microsats or even nanosats, to perform specific tasks. Some missions will use solar electric propulsion (SEP) instead of rockets. CIGS2 thin-film solar cells on flexible foil substrates may be able to increase the specific power by an order of magnitude from the current level of 65 W/kg.Thin film technology could conservatively reduce the array-manufacturing cost of a medium-sized 5-kW satellite from the current level of $2000k to less than $500k [8]. Non-rigid cells also have an advantage in stability. Because of the low initial velocities and steady acceleration, SEP satellites must spend long periods in intense regions of trapped radiation belts. CIGS solar cells are superior to the conventional silicon and gallium arsenide solar cells in the space radiation environment. The potential for improved radiation resistance of thin-film solar cells relative to single-crystal cells could extend mission lifetimes substantially. Recent studies have shown that 12.6% efficient, thin-film cells would start to become cost-competitive in geosynchronous earth orbit (GEO) and low earth orbit (LEO) missions [9].

The objective of the present research is to develop lightweight, radiation-resistant, highly efficient, high-specific-power CIGS thin-film solar cells for space electric power.

Metallic precursors, CuGa/In are deposited by DC magnetron sputtering on 10 cm x 10 cm substrate area. A small proportion of gallium is incorporated so as to obtain benefits of improved adhesion, slightly higher bandgap, and incorporation of a back-surface field, as has been done with CIGS cells on conventional substrate. Initially, CIGS2 thin-film solar cells are being fabricated on 127-μm-thick SS substrates. A few CIGS2 cells have also been prepared on 20-μm-thick SS substrates. CdS heterojunction partner is deposited by chemical bath deposition. Intrinsic ZnO and aluminum doped ZnO is deposited by RF magnetron sputtering. Sputtering technique that is used in the preparation of solar cell provides an added advantage of facilitating easy scale-up of the laboratory size cells to the commercially available size manufactured in industries using the roll-to-roll process. Cells are completed by depositing Ni/Al front contact fingers by thermal evaporation. CIGSeS and CIGS2 thin films were analyzed by scanning electron microscope to study the nature of morphology including grain size and compactness of the film. X-ray diffraction was carried out during the series of experiments to optimize the deposition and selenization/sulfurization parameters. Energy dispersive spectroscopy was used to study the stoichiometric composition. Auger electron spectroscopy was carried out to verify the elemental variation along the thickness of the film. Transmission electron microscopy was also carried out to study the active mechanisms at the interface hampering the efficiency of the cell. Best efficiency of 8.84% under AM 0 conditions and 10.4% under AM 1.5 conditions was achieved on 2.5 cm x 2.5 cm stainless steel substrate from a cell of 0.4 cm^2 total area. However, significant technological hurdles remain before thin-film technology could be implemented as the primary power source for spacecraft.

2. Experimental work

A 25 μm thick Ti substrate of was used as substrate. It can provide specific power of 1015 W/Kg with a 10% efficient cell. It was coated with a dielectric barrier layer of SiO_2 using sol-gel dip coating method. Sol-gel was prepared in two steps. First, alkoxide and ethanol were mixed in 1:5 proportions. In the second step, distilled-deionized water and acid were added to obtain final alkoxide:ethanol:H_2O:acid ratios of 1:5:5.1:0.55. The solution was stirred and preserved in a large beaker for 24 hours for the reaction to complete [10]. The substrates were completely immersed in sol-gel and then withdrawn at a well-defined speed under controlled thermal and atmospheric conditions. The uniformity of coating thickness depends on precise speed control and minimal vibration of the substrate and fluid surface. The coated substrate was sintered at $450^{o}C$ for 1 hour to form a uniform coating. The surface roughness was observed to improve from average roughness (R_a) 1750 Å to 542 Å. Bright annealed stainless steel foils with thickness of 127 μm and 20 μm were also used as substrates. CIGS2 thin films were prepared by a two-step process. The first step consisted of sputter- deposition of alternate layers of CuGa(22%) and In, to achieve the elemental ratio of Cu/(In+Ga) ~1.4, on a molybdenum-coated flexible foil substrate. This formed a stacked elemental layer sequence that produced a predominant $Cu_{11}In_9$ precursor phase. This layer was sulfurized in Ar:H_2S 1:0.04 gas mixture and argon flow rate of 650 sccm, using a three zone furnace. The temperature of initial dwell was changed from 120 to 135°C. After annealing the samples in flowing argon for 25 min at

this temperature, the flow of H_2S gas was initiated. The maximum sulfurization temperature was 475°C, while the sulfurization time was varied from 20 to 60 min. It was found that the binary $Cu_{11}In_9$ precursor phase reacted in the H_2S:Ar gas environment to form a good crystalline pseudo-quaternary phase of CIGS2 film. Some samples were sulfurized at 475°C for 30 min, followed by annealing at 500°C without H_2S gas flow in an Ar atmosphere for 10 min. This annealing step favored grain growth and recrystallization. The Cu-rich stoichiometry during the growth of CIGS2 films results in an improved morphology, i.e., enhanced grain sizes of the polycrystalline films through a pseudo-liquid Cu-S phase. For the sulfur system, according to the phase diagram of Cu–S, the respective liquid phase is not expected in the substrate temperature range of T_{sub}<600°C. However, owing to the high cation mobility in the Cu–S compounds, the cation lattice in a binary Cu–S phase at the surface of a growing CIS2 film behaves as a quasi-liquid. For selenide system, this phenomenon is attributed to CuSe liquid formed on top of Cu-rich films [11]. The Cu_xS phase was etched in 10% aqueous KCN solution. Solar cells were completed by deposition of CdS heterojunction partner layer by chemical bath deposition, and deposition of transparent-conducting i:ZnO/ZnO:Al window bilayer by RF sputtering, and vacuum evaporation of Ni/Al contact fingers through a metal mask (Figure 1). Bright annealed stainless steel foils of 20 and 127 μm thicknesses were evaluated among possible substrate materials for polycrystalline CIGS2 solar cell.

The deposition sequence was on flexible Ti foils was SiO_2/Ti/SiO_2/CIGSeS/CdS/i:ZnO/ZnO:Al/Ni/Al. Mo back contact and Cu-Ga-In metallic precursors were deposited by DC magnetron sputtering. Mo being a refractory material develops stress depending upon the sputtering power and pressure. Mo was deposited using a three-layer sequence. The Mo layer with tensile stress was sandwiched between two layers with compressive stress to reduce the overall stress and to build a 500 nm thick layer.

CuGa was deposited at 350 watts and 1.5×10^{-3} Torr argon pressure while indium was deposited at 230 watts and $7x10^{-4}$ Torr argon pressure. The time of deposition of each layer was adjusted so as to obtain 2.75 μm thickness of the absorber layer. The elemental stack was selenized at 400°C for 10 minutes followed by sulfurization at 475°C for 20 minutes. The cells were completed by depositing CdS, n-type hetero-junction partner layer by chemical bath deposition, and deposition of window bilayer of i:ZnO and ZnO:Al by RF magnetron sputtering and Ni/Al contact fingers by e-beam evaporation.

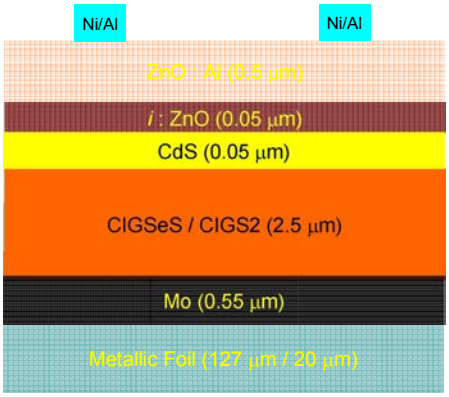

Figure 1. Layer sequence of CIGS2 thin film-solar cell

The phases, surface morphologies and elemental depth profiles of the CIGS2 films prepared on stainless steel flexible foils substrates were characterized as follows: Films were examined visually for their appearance, color and any tendency to peeling. X-ray diffraction (XRD) was used to identify the crystalline phases, using a RIGAKU diffractometer. The 2θ-range for the diffractometer was set from 10 to 80° with a step size of ?0.02°. Surface morphology of the CIGS2 thin film was studied using scanning electron microscopy (SEM). Chemical composition was analyzed by electron probe microanalysis (EPMA). Depth profiling was performed by secondary ion mass spectroscopy (SIMS) and Auger electron spectroscopy (AES) with simultaneous sputter etching. The substrate surface roughness and thickness of thin films were measured using the surface profile measuring system. Current–voltage characteristics of CIGS2 solar cells were measured under AM0 and AM1.5 conditions at the NASA Glenn Research Center and National Renewable Energy Laboratory (NREL). Quantum efficiency was measured at NREL.

3. Results and Discussion

The scanning electron microscopy (SEM) micrograph of CIGSeS film on Ti foil in Figure 2 shows compact CIGSeS grains with grain size of approximately 1 to 2 μm. Table I provides the elemental concentrations of CIGSeS thin film on Ti foil obtained using X-ray energy dispersive spectroscopy (XEDS) at 15 KV. It was observed that the amount of gallium was high while the film was copper-poor. These observations are also supported by X-ray diffraction (XRD) analysis. The shift of peaks towards higher 2θ value indicates high gallium content. XRD analysis (Figure 3) confirmed the presence of a chalcopyrite structure with (112)

preferred orientation. Intensity ratio of planes 112/220 was 3.7.

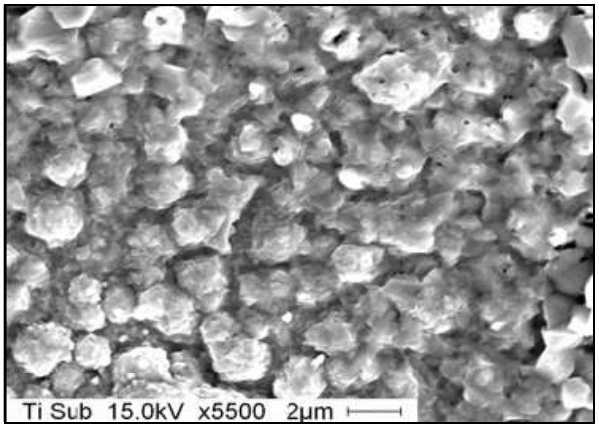

Figure 2. SEM of CIGSeS film on Ti foil at 5500 X

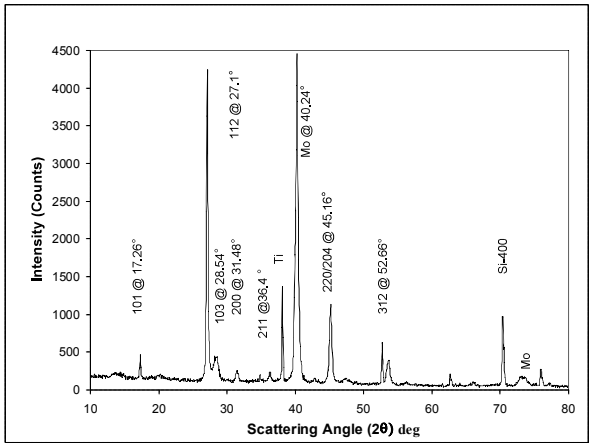

Figure 3. XRD Pattern of CIGSeS on Ti foil.

Table 1. XEDS of CIGSeS film on Ti foil analysis at 15kV

Element	Cu	In	Ga	Se	S
At %	23.26	21.60	7.41	20	27.72

Auger electron spectroscopy (AES) analysis of CIGSeS film on Ti foil showed that the gallium concentration increases towards the back contact while that of indium decreases. Gallium has a tendency to diffuse towards the back contact. It is also seen that the sulfur concentration is higher that that of selenium along the thickness of the film which is in accordance with the XEDS data. Higher amount of sulfur in the film indicated that the selenization was not complete and the film had substantial amount of selenium vacancies. These vacancies were filled up during post sulfurization by sulfur atoms. Further experiments were carried out on Mo-coated glass to establish the requisite temperature for complete selenization of the film. It was found that selenization at 500°C resulted in complete dissociation of diethyl selenium, providing adequate selenium to go in the film. Further experiments will be carried out on Ti foil at 500°C to study the adhesion and morphology of CIGSeS films.

For CIGS2 thin films on stainless steel (SS) foils, the initial dwell of 30 min at 120°C was changed to 135°C, and the flow of H_2S gas was started after 25 min at 135°C to avoid the formation of voids before the initiation of sulfurization [12]. The XRD spectrum of the as deposited (Cu+Ga)/In metallic precursors processed at 135°C indicated the presence of a highly oriented $Cu_{11}In_9$ phase without any elemental or alloy phases. The XRD pattern of a near stoichiometric, slightly Cu-poor, etched CIGS2 thin film on SS foil is shown in Figure 4; it showed (101), (112), (103), (004)/(200), (213),(204)/(200), (116)/(312), (008)/(400), and (332) reflections of a $CuIn_{0.7}Ga_{0.3}S_2$ phase. The calculated lattice parameters were a = 5.67 Å and c = 11.34 Å. A Mo peak was obtained at 40.22°. The (112) peak of $CuGaS_2$ was also observed. This is attributed to Ga diffusion towards the Mo back-contact, creating a Ga-rich phase near the back, and a Ga-poor phase at the surface and in the bulk of the CIGS2 thin film [13]. In the case of random orientation, the intensity ratio of (112) with respect to (220)/(204) peaks, should be 1.5. The intensity ratio of $I_{112}/I_{220/204}$, for these films, was remarkably higher, showing a high degree of (112) preferred orientation.

It may be noted that (112) orientation would be beneficial for achieving a good lattice match with CdS, and consequently for efficient device fabrication. Despite the very Cu-rich film of the unetched sample, with Cu/(In+Ga) ratio up to 1.68, no secondary phases could be detected in the XRD pattern for the unetched sample [14]. As discussed earlier, a Cu-rich stoichiometry during the growth of CIGS2 films results in an improved morphology i.e. enhanced grain size of the polycrystalline films. This excess Cu_xS was etched in 10% KCN solution.

The scanning electron micrograph (SEM) of a near stoichiometric, slightly Cu-poor, etched CIGS2 thin film on SS foil is shown in Figure 5. SEM image for the sample showed large, well-faceted grains with slight porosity. The porosity was observed at the grain boundaries from where the Cu_xS phases have been etched. The grain size measured by an intercept method was 3 µm i.e., comparable to the film thickness.

An AES survey (Figure 6) of near stoichiometric, slightly Cu-poor, etched CIGS2 thin film sample on SS foil, was performed over a range of kinetic

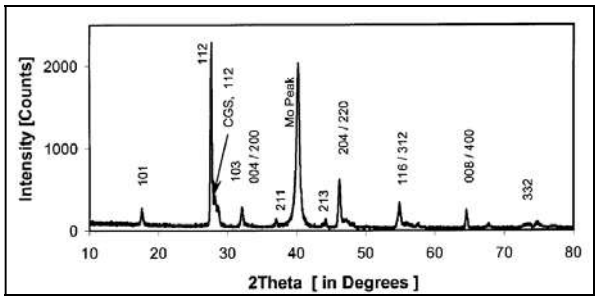

Figure 4. XRD pattern from a near stoichiometric, slightly Cu-poor, etched CIGS2 thin film on SS foil.

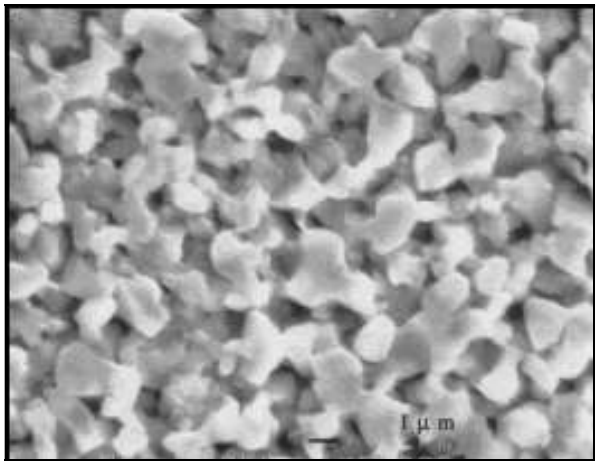

Figure 5. SEM image of a near stoichiometric, slightly Cu-poor, etched CIGS2 thin film on SS foil.

energies (50–2250 eV), using the primary electron beam of energy 5 keV. A representative area of sample was chosen and an AES survey was carried out at magnification of 1000X, equivalent to an area of 102X102 µm. An AES survey over the selected area showed the presence of copper at 60, 777, 850, and 924 eV, sulfur at 151, and 2131 eV, indium at 345 and 410 eV, gallium at 1071 eV, carbon at 273 eV, potassium at 252 eV and oxygen at 515 eV. The surface atomic concentrations calculated from the peak to peak height from the AES survey and relative sensitivities of the respective elements were as follows: copper 20.67 at. %, sulfur 31.62 at. %, indium 12.3 at.%, gallium 6.92 at.%, potassium 7.72 at.%, oxygen 11.92 at.% and carbon 15.04 at %.

The AES depth profile was obtained by sputtering an area of 1x1mm^2 with energetic argon ions at a rate of 475 Å /min for 72 min. Figure 7 shows peak heights at ifferent depths (time) for different elements. The peak heights were obtained for the following elements: copper, indium, gallium, oxygen, carbon, sulfur, molybdenum, iron and potassium. Copper and sulfur

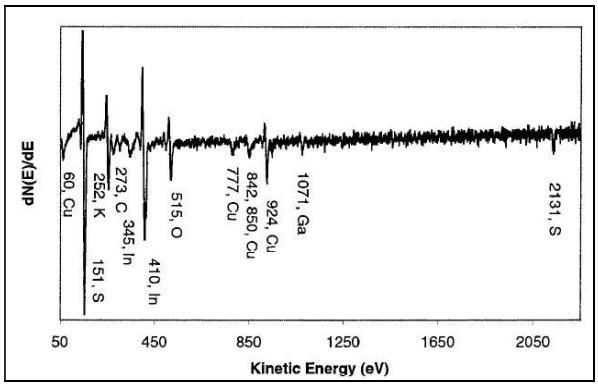

Figure 6. Surface AES survey of near stoichiometric, slightly Cu-poor, etched CIGS2 thin film on SS foil.

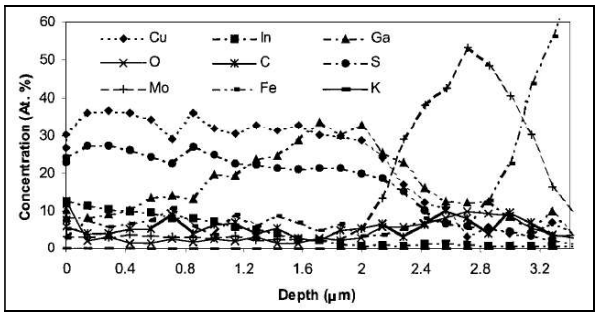

Figure 7. AES depth profile of near stoichiometric, slightly Cu-poor, etched CIGS2 thin film on SS foil.

concentration showed the same trend; it decreased near the Mo back-contact. Potassium was detected at the surface. Its concentration decreased rapidly in the bulk. Potassium was attributed to the KCN treatment that was used to etch away excess Cu_xS phase. Indium concentration was constant in most of the thickness of CIGS2 layer, then decreased with depth becoming negligible at the CIGS/Mo interface. Concentration of gallium at the surface was approximately 10%, while at the CIGS/Mo interface it was 30%. This showed that Ga concentration increased towards the Mo back-contact. Beyond the thickness of the Mo back-contact layer, the concentration of iron rises, due to iron in the stainless steel foil. The apparent concentration of iron within the CIGS2 film thickness would create an erroneous impression of iron diffusion. This is discussed further below. Apparent humps in the depth profiles were caused by a non-uniform sputter-etching rate. It can be seen that the film thickness of etched CIGS2 sample from the depth profile was approximately 2.4 µm.

SIMS depth profiling (Figure 8) of CIGS2 film on SS foil was performed on an etched sample by positive

SIMS, using a CAMECA IMS-3F system with oxygen primary beam current 150 nA, impact energy 5.5 keV, angle of incidence 42°, rastered over 250x250 μm, with source at 10 keV and sample at 4.5 keV. The corresponding unetched sample had Cu/(In+Ga) ~1.4, and was sulfurized at 475°C for 30 min, and annealed for 10 min each at 475 and 500°C. The slightly Cu-poor, etched CIGS2 thin-film sample was monitored for eight species. To achieve high sensitivity measurements, secondary positive cluster ions such as ^{23}Na, ^{34}S, K, ^{54}Fe, ^{65}Cu, (^{69}Ga+O), ^{92}Mo,and (^{113}In+O) were used for detection of Na, S, K, Fe, Cu, Ga, Mo, and In respectively. Cu concentration was mostly constant over the depth of the film. Ga concentration remained constant to 1 μm, and then increased to the Mo back-contact. Indium concentration remained constant through most of film thickness and decreased near the Mo back-contact. Na was not added intentionally. S concentration was uniform throughout film thickness. Na concentration at the surface of the substrate was attributed to the residue from cleaning with soap solution. Potassium incorporation was due to etching of the Cu_xS phase present on the grains and near the grain boundaries with KCN solution. Careful SIMS analysis, described below, showed that the concentration of iron was below the detection limit. Thus there was no significant diffusion of iron. No sharp interfaces were observed at CIGS2/Mo and Mo/substrate. This was probably because of the interdiffusion of species and porosity formed due to etching with 10% KCN treatment.

The mass spectrum recorded from masses of 1–120 is shown in Figure 8. Sharp peaks were observed for elemental and molecular species such as O_2^+, S^+, K^+, Ca^+, SO^+, Cu^+, Ga^+, GaO^+, CuO^+, CuO^{2+}, In+, InO^+, and InO_2^+ . Na was not detected during analysis of mass spectra. Because of the large number of isotopes of Cu, In, Mo, Ga, and S, a number of mass interferences were observed. The mass spectrum clearly indicated the presence of Cu, In, Ga, S, Mo and K. The chemical composition of CIGS2 films on SS foils was analyzed by EPMA. Average atomic concentrations measured at 10 kV and 20 kV for an unetched sample showed Cu:In:Ga:S proportion of 51.52:7.80:1.83:38.83 and 41.90:10.92:2.56:44.63, respectively. The Cu:In:Ga:S atomic concentrations for the etched sample at 10 and 20 kV were found to be 27.38:21.61:3.30:47.71 and 23.96:19.36:5.70:50.99, respectively. The compound formulae were $Cu_{1.09}In_{0.87}Ga_{0.13}S_2$ and $Cu_{0.96}In_{0.77}Ga_{0.23}S_2$, respectively. The Cu:In:Ga:S atomic concentrations for the etched sample deposited on 20-μm-thick SS foil at 20 kV were found to be 28.60: 14.90:11.42:45.10. The compound formula was $Cu_{1.10}In_{0.60}Ga_{0.40}S_2$.

Surface roughness of the substrate was measured with the surface profile measuring system. The average roughness, R_a value for 127-μm-thick SS foil (Figure 9) was 62.3 Å and average waviness W_a was 141.6 Å. The average roughness Ra for 20-μm-thick SS foil (Figure 10) was 396.4 Å and surface waviness W_a was 773.2 Å.

PV parameters of a CIGS2 solar cell on 127-μm-thick SS flexible foil measured under AM0 conditions (Figure 11) at NASA GRC were: open-circuit voltage, V_{OC} = 802.9 mV, short-circuit current density, J_{SC} = 25.07 mA/cm^2, fill factor, FF = 60.06%, and efficiency η = 8.84%. For this cell, AM1.5 PV parameters measured at NREL were: open-circuit voltage, V_{OC} = 763 mV, short-circuit current density, J_{SC}= 20.26 mA/cm^2, fill factor, FF = 67.04%, and efficiency η = 10.4%. The quantum efficiency curve (Figure 12) showed a sharp QE cut-off, equivalent to a CIGS2 bandgap of ~1.50 eV, fairly close to the optimum value for efficient AM0 PV conversion in space. PV parameters for a cell fabricated on 20-μm-thick SS foil measured at NREL under AM1.5 conditions were: V_{OC}=740mV, J_{SC}=13.129 mA/cm^2, FF = 41.63%, and η = 4.06%.

Foils with high defect density, in the form of surface roughness, showed an increase in Ga content in the bulk of material. Fill factor, i.e., the squareness of the I–V curve also decreased with increase in defect density. Efficiency showed a decreasing trend with increasing surface roughness. The loss in efficiency was attributed to surface roughness of the substrate, and decrease in fill factor. The solar efficiency of a photovoltaic system depends critically on the spectral distribution of the radiation.

At AM0 the solar spectrum has an irradiance of 1353 W/m^2. At the PV Materials Laboratory of FSEC, the goal is to achieve efficiency under AM0 conditions in the range of 10–15%. Table 2 provides the projected specific power in W/kg of flexible metallic substrate at AM0 for 10 and 15% efficient CIGS2 solar cells.

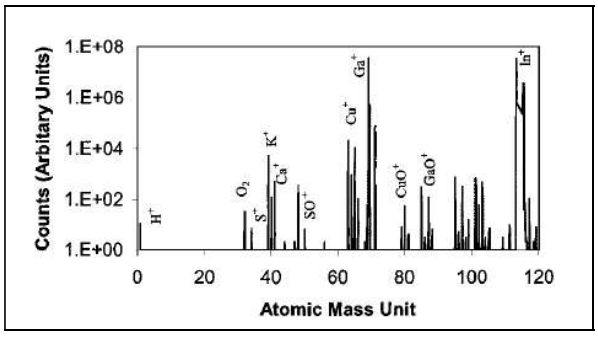

Figure 8. SIMS mass spectra of near stoichiometric, slightly Cu-poor, etched CIGS2 thin film

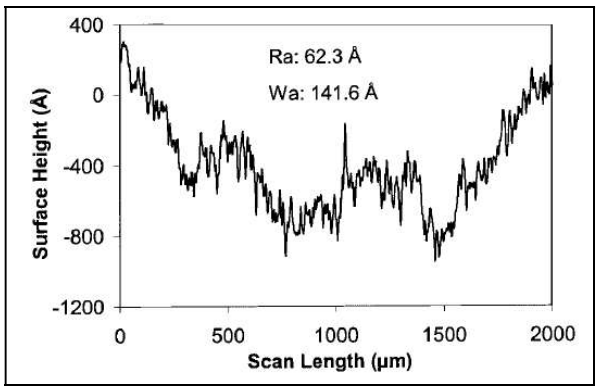

Figure 9. Surface roughness measurement of 127-mm-thick SS foil

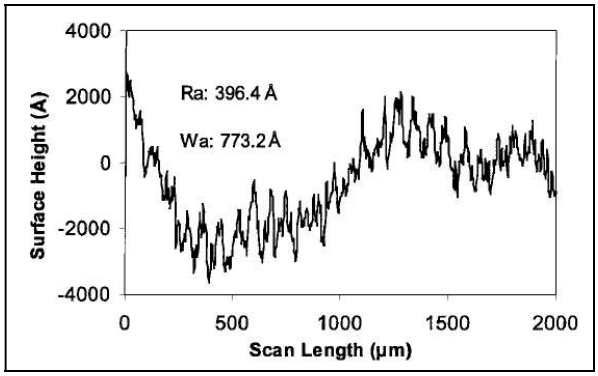

Figure 10. Surface roughness measurement of 20-mm-thick SS foil

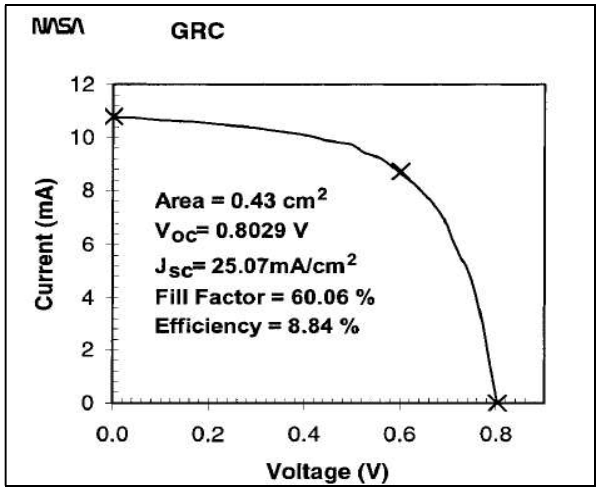

Figure 11. AM0 I–V curve of CIGS2 thin film solar cell (NASA GRC)

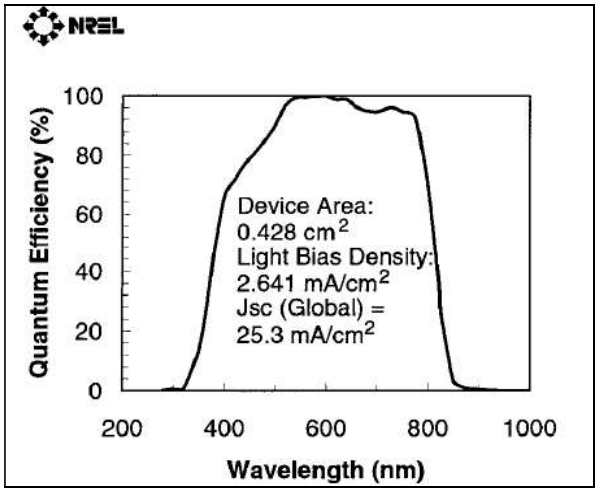

Figure 12. QE curve of CIGS2 thin film solar cell (NREL)

Table 2. Projected specific power for CIGS2 solar cells

Substrate	Projected specific power (W/kg)	
	η = 10% at AM0	η = 15% at AM0
127-µm (5 mil) SS foil	33.0	199.6
20-µm (< 1mil) SS foil	768.8	1153.1
25.4µm (1 mil) Ti foil	1015.8	1523.6

4. Conclusions and Future Plans

Flexible and ultra-lightweight SiO_2 coated Ti foil was used successfully as a substrate for preparing CIGS2/CdS thin-film solar cells using selenization/sulfurization of sputtered metallic precursors technique. Efficiencies above 10 % can be obtained by improving the growth behavior of CIGSeS layer and fine tuning the process, work is being continued on CIGSeS films as well. Further selenization using diethyl selenium of elemental stack will be carried out at higher temperature.

Sputtered copper, gallium and indium precursors with Cu/(In+Ga) ratio ~1.4 formed a predominant $Cu_{11}In_9$ precursor phase, free from inhomogeneous secondary phases. The temperature of the initial 30-min dwell of 120°C was changed to 135°C. H_2S gas flow was begun after 25 min of the dwell. The binary $Cu_{11}In_9$ precursor phase reacted in an H_2S: Ar gas environment to form a good crystalline pseudo-

quaternary phase of CIGS2 film. After etching in KCN, CIGS2 films became stoichiometric when the the ratio of Cu/(In+Ga) of unetched film was in the range 1.4-1.8. CIGS2 films grew with (112) texture of the chalcopyrite structure. A highly Ga-rich phase was formed near the back-contact while a Ga-poor phase was formed in the bulk of the film and in the electrically active part of the device, because of the tendency of gallium to diffuse towards the back-contact. The bandgap of this film was narrow at the surface and in the bulk, and widened towards back-contact, leading to formation of a back-surface field. This built-in back-surface electric field was expected to improve the solar cell performance [15, 16]. PV parameters of a CIGS2 solar cell on 127-µm-thick SS flexible foil measured under AM0 conditions at the NASA GRC were: V_{OC} = 802.9mV, J_{SC} = 25.07 mA/cm^2, FF = 60.06%, and η = 8.84%. For this cell, AM1.5 PV parameters measured at NREL were: V_{OC} = 763mV, JSC= 20.26mA/cm^2, FF = 67.04%, η = 10.4%. Quantum efficiency curve showed a sharp cut-off, equivalent to a CIGS2 bandgap of ~1.50 eV, fairly close to the optimum value for efficient AM0 PV conversion in space. PV parameters for a cell fabricated on 20-µm-thick SS foil measured at NREL under AM1.5 conditions were: V_{OC}=740mV, J_{SC}=13.129 mA/cm^2, FF = 41.63%, η = 4.06%.

Foils with high defect density in the form of surface roughness showed an increase in Ga content in the bulk of material. Fill factor, i.e., the squareness of the I–V curve also decreased with increase in defect density. Efficiency decreased with increasing surface roughness. With the construction of large-area, dual-chamber magnetron-sputtering unit, samples of thickness uniformity ±2% over the central 5 inch (12.5 cm) width and ±3% over the central 6 inch (15 cm) width will be fabricated.

5. Acknowledgements

This work was supported by the NASA Glenn Research Center, contract NCC 3712, the Air Force Research Laboratory through Jackson and Tull and Universities Space Research Association, contract 09503-01, and the National Renewable Energy Laboratory, contract NDJ-2-30630-03. The authors are thankful to Mr. Ken Zweibel, Dr. Harin Ullal, Dr. Bolko von Roedern, Dr. Helio Moutinho, Dr. Kannan Ramnathan, Tom Moriarty and Bobby To of NREL for help with Ni/Al grid deposition, I–V and QE measurements, and EPMA analysis and discussions.

6. References

[1] M. Contreras, K. Ramanathan, J. AbuShama, F. Hasoon, D. L. Young, B. Egaas and R. Noufi, Progress in Photovoltaics:Research and Applications, 2005, 13: 209-216.

[2] W. Hörig, H. Neumann and H. Sobotta B. Schumann and G. Kühn, Thin Solid Films, 48,1, 67-72, (1978)

[3] S. Zhang, S. Wei, A. Zunger, Physics review letter, 1997, 78: 4059–4062.

[4] A. Jasenek, U. Rau, K. Weinert, I. Kötschaua, G. Hannaa, G. Voorwinden, M. Powalla, H. Schock and J. H. Werner, Thin Solid Films, 2001, 387: 228–230.

[5] W. Batchelor, I. Repins, J. Schaefer, and M. Beck, Solar Energy Materials & Solar Cells, 2004, 83: 67–80.

[6] T. Nakada, H. Ohbo, T. Watanabe, H. Nakazawa, M. Matsui, and A. Kunioka, Solar Energy Materials and Solar Cells, 1997, 49: 285-290.

[7] Satoh T, Hashimoto Y, Shimakawa S-i, Hayashi S, Negami T. Proceedings of the 28th IEEE Photovoltaic Specialists Conference, Anchorage, 2000; 567–570.

[8] Ralph EL, Woike TW. Proceedings of the 37th American Institute of Aeronautics and Astronautics Aerospace Sciences Meeting and Exhibition 1999; 1–7.

[9] Tringe J, Merrill J, Reinhardt K. Proceedings of the 28th IEEE Photovoltaic Specialists Conference, Anchorage, 2000; 1242–1245.

[10] N. Dhere, V. Gade and S. Kulkarni, Proceedings of 3rd World Conference on Photovoltaic Energy Conversion, Osaka, Japan, 2003.

[11] Scheer R, Lewerenz HJ.Journal of Vacuum Science Technology 1995; A13(4): 1924–1929.

[12] Miles RW, Reddy KTR, Forbes I. Proceedings of the 2nd World Conference on Photovoltaic Solar Energy Conversion, Vienna, 1998; 496–499.

[13] Klaer J, Neisser JA, Hengel I, Klenk R, Matthes ThW, Garcia JA, Rodriguez AP, Rodriguez AR, Stenier MCh. Solar Energy Materials and Solar Cells 2001; 67:97–104.

[14] Dhere NG, Kulkarni SR, Chavan SS, Ghongadi SR. Proceedings of the 16th Space Photovoltaics Research and Technology Conference, Cleveland, 1999.

[15] Dhere NG, Kulkarni SR, Ghongadi SR. Proceedings of the 28th IEEE Photovoltaic Specialists Conference, Anchorage, 2000; 1046–1049.

[16] Dhere NG, Kulkarni SR, Johnson PK. Proceedings of the 16th European Photovoltaic Solar Energy Conference, Glasgow, 2000; 1–4.

FLORIDA SOLAR ENERGY CENTER

Creating Energy Independence Since 1975

CIGSeS and CIGS2 Thin Film Solar Cells on Flexible Foils for Space Power

Neelkanth G. Dhere, Sachin S. Kulkarni, Shirish A. Pethe, Vinay V. Hadagali, Parag S. Vasekar

A Research Institute of the University of Central Florida

Introduction

Requirements of space power

- Lightweight
- Radiation resistant
- Highly efficient
- High specific power

Introduction

- CIGS and CIGS2 as ideal candidates
  - Can be fabricated on lightweight substrates such as stainless steel (SS) or titanium foils
  - Highest conversion efficiency of all thin film technologies
  - Higher radiation resistance as compared to crystalline silicon solar cells
  - Increase in specific power by over an order of magnitude from current level of 65 W/kg

Introduction

- Selection criteria for substrate
  - Thermal expansion
  - Chemical effect or the diffusion of detrimental impurities in the absorber layer
  - The influence of surface properties on nucleation
- Titanium foil a potential candidate
  - Thermal coefficient of $8.6\times10^{-6}/^{o}C$
  - Deposition of SiO_2 prevents diffusion of impurities

Thin Film Solar Cell Structure

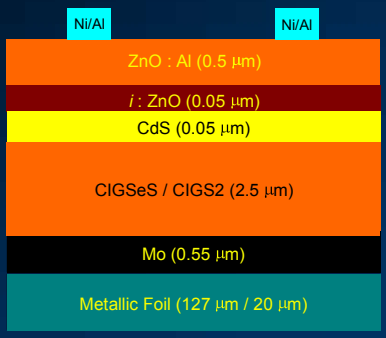

Experimental Work

- 25 μm thick Ti substrate was used – specific power of 1015 W/kg for 10% efficient cell
- SiO_2, dielectric barrier layer, deposited by Sol-gel process
- Deposition of metallic precursors using DC magnetron sputtering.

Experimental Work

- Sulfurization for CIGS2 [Cu/(In+Ga)~ 1.4]
  - The metallic precursors were annealed in Ar:H_2S mixture for 20 - 60 min at ~475°C
  - Some samples were further annealed at ~500°C in inert ambient for recrystallization and better grain growth

Experimental Work

- Selenization/Sulfurization for CIGSeS
  - The metallic precursor was selenized in H_2:DESe mixture at ~400°C for ~10 mins.
  - This is followed by sulfurization in Ar:H_2S mixture at ~475°C for ~20 mins.
- CdS, heterojunction partner, deposited by chemical bath deposition
- A window layer of i-ZnO / ZnO:Al bilayer deposited by RF magnetron sputtering
- Ni/Al Contact fingers are deposited by thermal evaporation

Material Characterization

- Scanning electron microscopy (SEM) for morphological analysis
- X ray diffraction (XRD) analysis for crystallinity of the films
- X ray Energy dispersive spectroscopy (XEDS) and secondary ion mass spectroscopy (SIMS) for composition
- Auger electron spectroscopy (AES) for depth profile
- Transmission electron microscopy (TEM) to understand the interface properties

Electrical Characterization

- Current-Voltage (I-V) characteristics to determine the photovoltaic parameters: open circuit voltage (V_{oc}), short circuit current (I_{sc}), and fill factor (FF)
- Quantum efficiency (QE) analysis to understand the loss mechanisms over the complete solar spectrum

Result and Discussions

CIGS2 Absorber Film

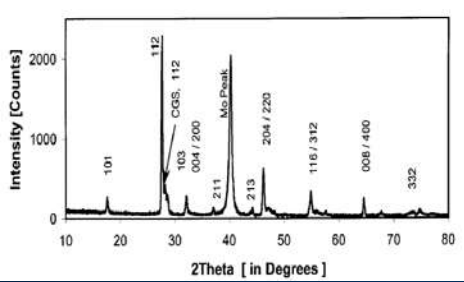

XRD pattern of a near stoichiometric, slightly Cu-poor, etched CIGS2 thin film on SS foil

- (101), (112), (103), (004)/(200), (213), (204)/(200), (116)/(312), (008)/(400), and (332) reflections of a $CuIn_{0.7}Ga_{0.3}S_2$ phase
- Calculated lattice parameters were a = 5.67 Å and c = 11.34 Å
- (112) peak of CuGaS2 was also observed - Ga diffusion towards the Mo back-contact, creating a Ga-rich phase near the back
- High degree of (112) preferred orientation

CIGS2 Absorber Film

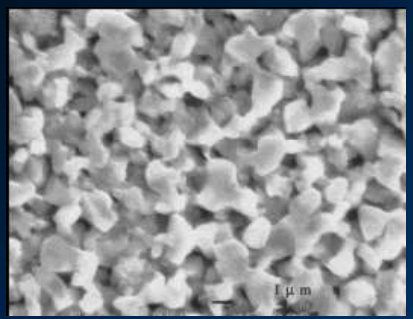

SEM image of a near stoichiometric, slightly Cu-poor, etched CIGS2 thin film on SS foil

- Large, well-faceted grains with slight porosity
- Porosity was observed at the grain boundaries from where the Cu_xS phases have been etched
- Grain size measured by an intercept method was ~3 μm

CIGS2 Absorber Film

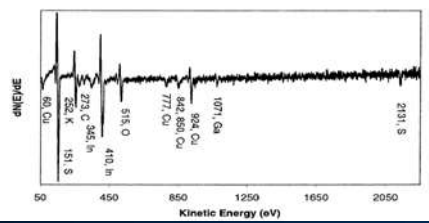

Surface AES Survey

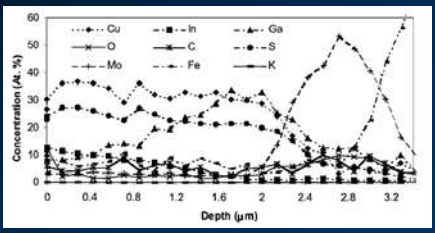

AES Depth Profile

- Calculated surface atomic concentrations:
  Cu - 20.67 at.%, S - 31.62 at. %, In - 12.3 at.%, Ga - 6.92 at.%, K - 7.72 at.%, O_2 - 11.92 at.% and C - 15.04 at %
- Cu and S concentration showed the same trend; it decreased near the Mo back-contact
- K detected at the surface and it decreased rapidly in the bulk
- Indium concentration was constant in the bulk and reduced at the Mo back-contact
- Ga concentration was low in the bulk and increased near the Mo back-contact

CIGS2 Absorber Film

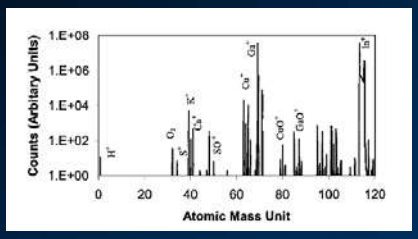

SIMS mass spectra of near stoichiometric, slightly Cu-poor, etched CIGS2 thin film

- The mass spectrum clearly indicated the presence of Cu, In, Ga, S, Mo and K
- Cu concentration was mostly constant over the depth of the film
- Ga concentration remained constant to 1 μm, and then increased to the Mo back-contact
- Indium concentration remained constant through most of film thickness and decreased near the Mo back-contact
- Sulfur concentration was uniform throughout film thickness
- Sodium concentration at the surface of the substrate was attributed to the residue from cleaning with soap solution

CIGS2 Absorber Film

EPMA analysis of an unetched CIGS2 sample

	Cu	In	Ga	S
10 kV	51.52	7.80	1.83	38.83
20 kV	41.90	10.92	2.56	44.63

compound formula was $Cu_{1.09}In_{0.87}Ga_{0.13}S_2$

EPMA analysis of etched CIGS2 sample

	Cu	In	Ga	S
10 kV	27.38	21.61	3.30	47.71
20 kV	23.96	19.36	5.70	50.99

compound formula was $Cu_{0.96}In_{0.77}Ga_{0.23}S_2$

EPMA analysis of etched sample deposited on 20- μ m-thick SS foil

	Cu	In	Ga	S
20 kV	28.60	14.90	11.42	45.10

compound formula was $Cu_{1.10}In_{0.60}Ga_{0.40}S_2$

CIGS2 Absorber Film

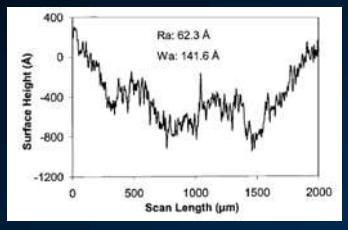

Surface roughness measurement of 127-mm-thick SS foil

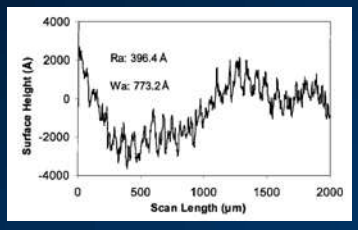

Surface roughness measurement of 20-mm-thick SS foil

- Foils with high defect density, in the form of surface roughness, showed an increase in Ga content in the bulk of material
- Fill factor also decreased with increase in defect density
- Efficiency showed a decreasing trend with increasing surface roughness

Light and Dark J vs V

☼ V_{oc} = 739 mV, J_{sc} = 26.01 mA/cm^2, FF = 63.7%, and η = 8.95%, under AM 0 conditions at NASA GRC

☼ J x V, IEC, Slight crossover >1.9xJ_{sc}

☼ Moderately photoconducting CdS layer.

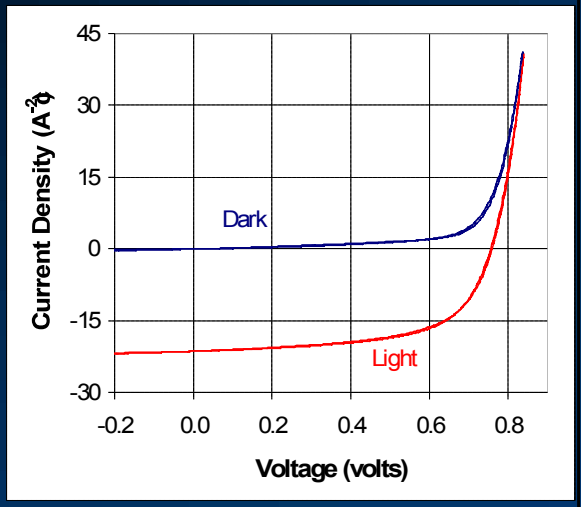

Light Curve Translation

☼ Light Current density (J + J_{sc}) and Dark Current density versus voltage

☼Light Curve Translation to check coincidence

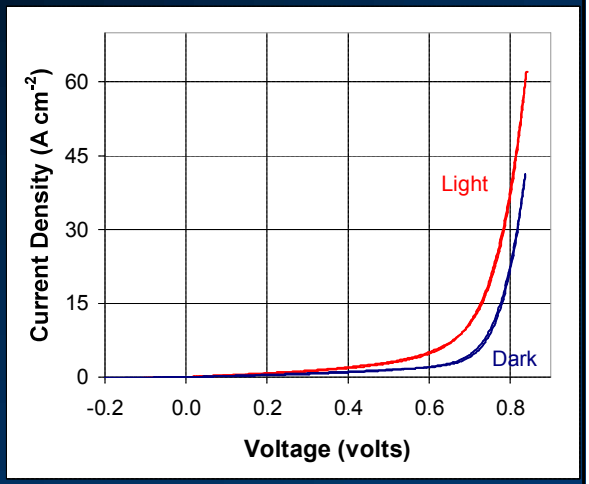

Log (J+Jsc) vs V_{total}

- Ascending and descending curves to verify hysteresis
- Main part, diode behavior
- Offset due to higher J_o under illumination
- Shunting effects <0.1 mA cm^{-2}
- No modification of slope due to Rs even at ~3x Jsc.

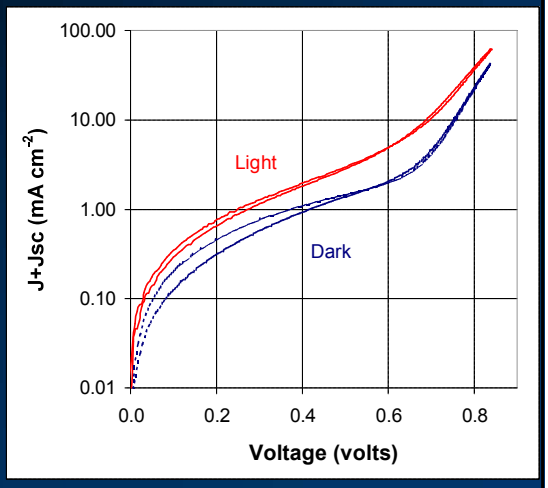

dJ/dV Vs Vs Voltage

- AC conductance by dJ/dV vs V around J_{sc}
- R_p ~600 Ω cm^2
- Xenon arc lamp flicker, noisy curve

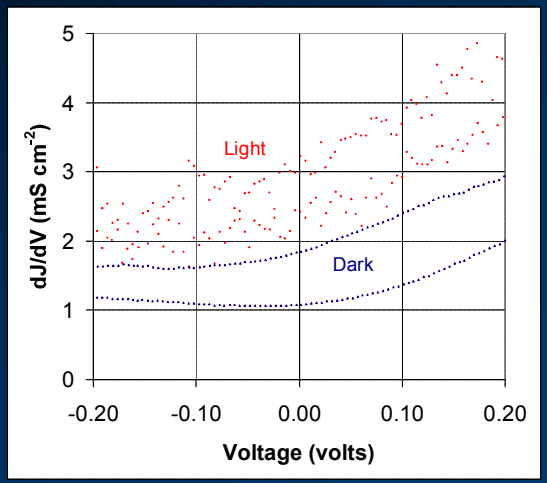

dV/dJ Vs 1/(J+Jsc)

- Straight lines - diode or exponential behavior
- Intercept at ∞
- Rs = 0.6 Ω
- Not essential to account for Rp
- Current loss by dV/dJ vs (1- (dV/(dJRp) [J+J_{sc}+V/Rp)]

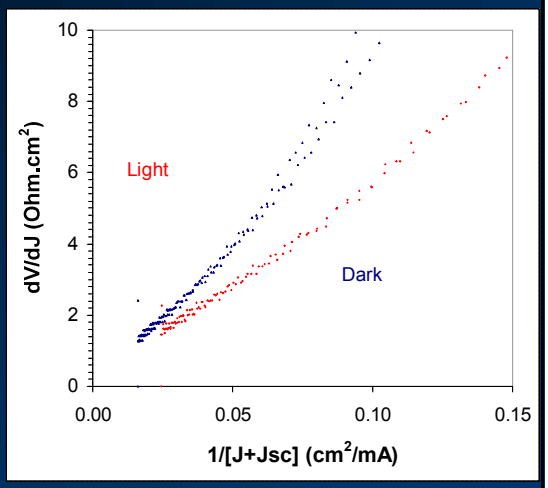

A and J_0 with Dark J

- Diode factor, A and reverse saturation current density, J_o from Ln (J+Jsc) vs corrected voltage V-RsJ
- J vs A & Ln J_o
- A ≈2.21 and J_o ≈ 1.85x10^{-8} A cm^{-2} wide dark J range

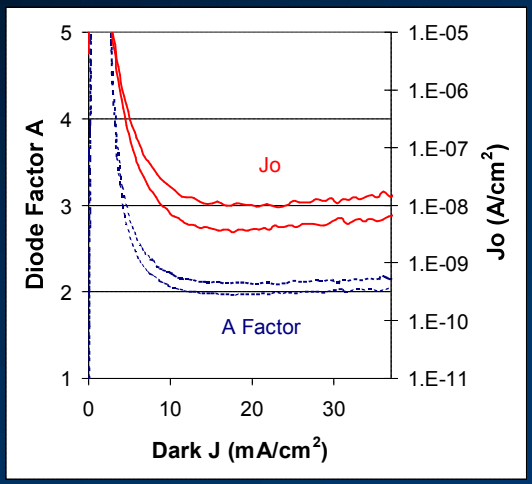

A^2/C^2 versus Voltage

☼ Extrapolation of the curve to $A^2/C^2 = 0$ gives the built-in-field V_d

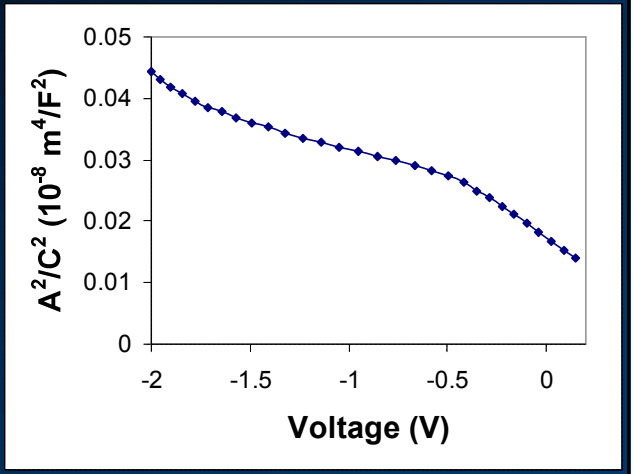

Dopant Density

☼Max. dopant density $N_A \sim 1.5 \times 10^{17}$ cm^{-3}

☼Junction width w = 0.15 μm

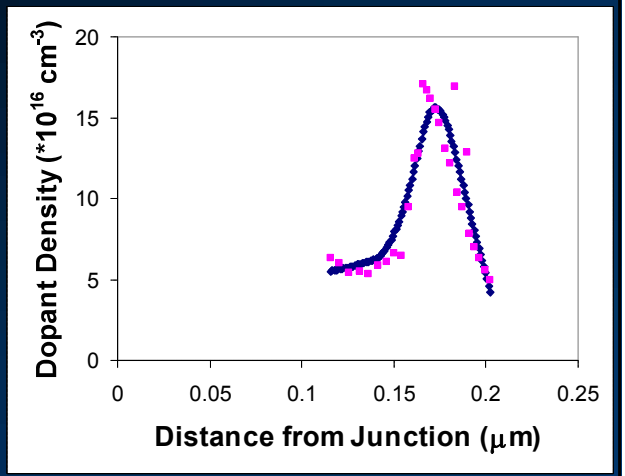

Conclusion

- Flexible and ultra-lightweight SiO_2 coated Ti foil was successfully used as a substrate for preparing CIGSeS/CdS thin-film solar cells using sputtering technique
- CIGS2 films grew with (112) texture of the chalcopyrite structure
- A highly Ga-rich phase was formed near the back-contact resulting in widened energy bandgap towards back-contact, leading to formation of a back-surface field

Conclusion

- PV parameters for a cell fabricated on 20-µm-thick SS foil measured at NREL under AM1.5 conditions were:

  V_{OC}=740mV, J_{SC}=13.129 mA/cm^2, FF = 41.63%, and η = 4.06%
- Efficiency decreased with increasing surface roughness

Conclusion

- PV parameters of a CIGS2 solar cell on 127-µm thick SS flexible foil measured under AM0 conditions at the NASA GRC were:

  V_{OC} = 802.9 mV, J_{SC} = 25.07 mA/cm^2, FF = 60.06%, and η = 8.84%
- PV parameters for same cell measured under AM1.5 conditions at NREL were:

  V_{OC} = 763 mV, J_{SC}= 20.26 mA/cm^2, FF = 67.04%, and η = 10.4%
- Quantum efficiency curve showed a sharp cut-off, equivalent to a CIGS2 bandgap of ~1.50 eV, fairly close to the optimum value for efficient AM0 PV conversion in space

Conclusion

- Various semiconducting properties such as Series resistance (R_s), Shunt resistance (R_p), Reverse saturation current density (J_o), Diode quality factor (A), and Doping density (N_A) were calculated using the measured photovoltaic parameters
- The calculated values were: R_s= 0.6 Ω/cm^2, R_p~600 Ω/cm^2, $J_o \approx 1.85 \times 10^{-8}$ A/cm^2, A ≈ 2.21, N_A ~1.5×10^{17} cm^{-3}, and Junction width (W) = 0.15 µm

Future Work

- Efficiencies above 10 % can be obtained by improving the growth behavior of absorber layer and fine tuning the process
- Further selenization using diethyl selenium of elemental stack will be carried out at higher temperature

Acknowledgement

- This work was supported by the NASA Glenn Research Center, contract NCC 3712, the Air Force Research Laboratory through Jackson and Tull and Universities Space Research Association, contract 09503-01, and the National Renewable Energy Laboratory, contract NDJ-2-30630-03
- The authors are thankful to Mr. Ken Zweibel, Dr. Harin Ullal, Dr. Bolko von Roedern, Dr. Helio Moutinho, Dr. Kannan Ramnathan, Tom Moriarty and Bobby To of NREL for help with Ni/Al grid deposition, I–V and QE measurements, and EPMA analysis and discussions